ARTICLE

HemaSphere ★EHA★ EUROPEAN HEMATOLOGY ASSOCIATION

Combined inhibition of CTPS1 and ATR is a metabolic vulnerability in p53-deficient myeloma cells

Romane Durand[1] | Céline Bellanger[1,^] | Géraldine Descamps[1,^] | Christelle Dousset[1,^] | Sophie Maïga[1,^] | Jennifer Derrien[1] | Laura Thirouard[1] | Louise Bouard[1] | Hélène Asnagli[2] | Philip Beer[2] | Andrew Parker[2] | Patricia Gomez-Bougie[1] | Marie-Claire Devilder[1] | Philippe Moreau[1] | Cyrille Touzeau[1] | Agnès Moreau-Aubry[1] | David Chiron[1] | Catherine Pellat-Deceunynck[1]

Graphical Abstract
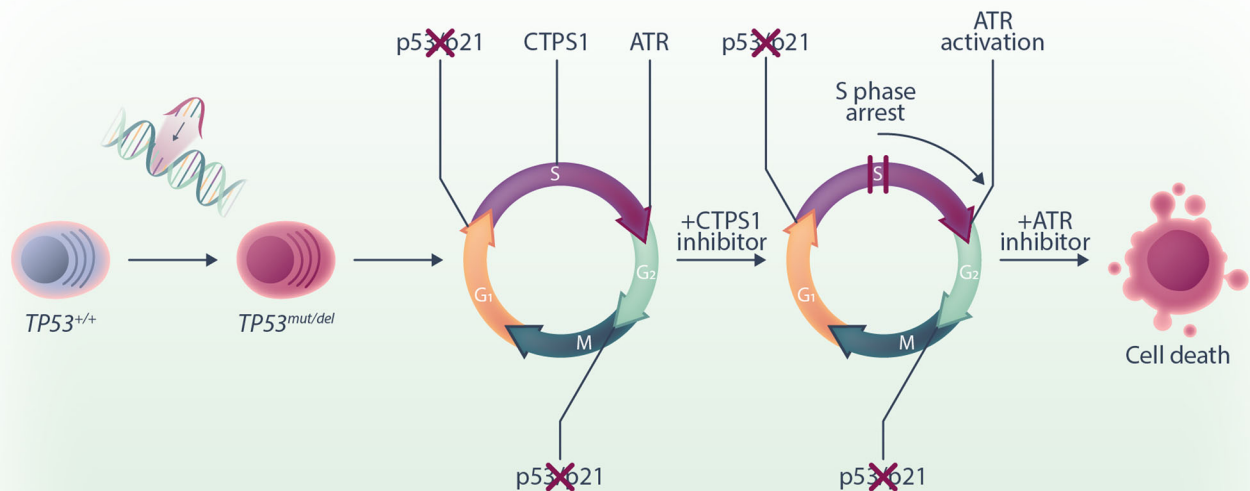
ARTICLE

HemaSphere ★EHA EUROPEAN HEMATOLOGY ASSOCIATION

Combined inhibition of CTPS1 and ATR is a metabolic vulnerability in p53-deficient myeloma cells

Romane Durand[1] | Céline Bellanger[1,^] | Géraldine Descamps[1,^] | Christelle Dousset[1,^] | Sophie Maïga[1,^] | Jennifer Derrien[1] | Laura Thirouard[1] | Louise Bouard[1] | Hélène Asnagli[2] | Philip Beer[2] | Andrew Parker[2] | Patricia Gomez-Bougie[1] | Marie-Claire Devilder[1] | Philippe Moreau[1] | Cyrille Touzeau[1] | Agnès Moreau-Aubry[1] | David Chiron[1] | Catherine Pellat-Deceunynck[1]

Correspondence: Catherine Pellat-Deceunynck (catherine.pellat-deceunynck@univ-nantes.fr)

Abstract

In multiple myeloma, as in B-cell malignancies, mono- and especially bi-allelic *TP53* gene inactivation is a high-risk factor for treatment resistance, and there are currently no therapies specifically targeting p53 deficiency. In this study, we evaluated if the loss of cell cycle control in p53-deficient myeloma cells would confer a metabolically actionable vulnerability. We show that CTP synthase 1 (*CTPS1*), which encodes a CTP synthesis rate-limiting enzyme essential for DNA and RNA synthesis in lymphoid cells, is overexpressed in samples from myeloma patients displaying a high proliferation rate (high *MKI67* expression) or a low p53 score (synonymous with *TP53* deletion and/or mutation). This overexpression of *CTPS1* was associated with reduced survival in two cohorts. Using scRNA-seq analysis in 24 patient samples, we further demonstrate that myeloma cells in the S or G2/M phase display high *CTPS1* expression. Pharmacological inhibition of CTPS1 by STP-B induced cell cycle arrest in early S phase in isogenic NCI-H929 or XG7 *TP53*^+/+, *TP53*^−/−, and *TP53*^R175H/R175H cells and in a *TP53*^−/R123STOP patient sample. The functional annotation of transcriptional changes in 10 STP-B-treated myeloma cell lines revealed a decrease in protein translation and confirmed the blockade of cells into the S phase. The pharmacological inhibition of ATR, which governs the intrinsic S/G2 checkpoint, in STP-B-induced S-phase arrested cells synergistically induced cell death in *TP53*^+/+, *TP53*^−/−, and *TP53*^R175H/R175H isogenic cell lines (Bliss score >15). This combination induced replicative stress and caspase-mediated cell death and was highly effective in resistant/refractory patient samples with *TP53* deletion and/or mutation and in *TP53*^−/− NCI-H929 xenografted NOD-scid IL2Rgamma mice. Our in vitro, ex vivo, and in vivo data provide the rationale for combined CTPS1 and ATR inhibition for the treatment of p53-deficient patients.

INTRODUCTION

Over the past decade, impressive therapeutic progress has been made in the treatment of patients with multiple myeloma (MM), thanks to the introduction of antibodies (such as anti-CD38, drug conjugate, and bispecific) or the development of cell therapies.[1–5] These treatments have increased response rates and the duration of response, even in refractory/resistant patients. However, it remains unclear whether these new treatments will effectively overcome resistance in patients with *TP53* defects, characterized by the deletion of the 17p locus (del17p) and/or *TP53* mutation.[6] In the meantime, treatment better adapted to these patients is still needed, as serial relapses, after initially efficient treatment, ultimately lead to the selection of cells with a greater number of *TP53* hits.[7,8]

Abnormalities in *TP53* lead to the loss of p53 function, which is crucial for cellular response to stress.[9] While the loss of p53 response

---

^Céline Bellanger, Géraldine Descamps, Christelle Dousset, and Sophie Maïga contributed equally to this work.

is an advantage for cancer cells to escape apoptosis, it also reveals other vulnerabilities that can be targeted: cells with *TP53* hits indeed fail to survive stress such as viral infection, or massive exposure to ROS.[9–11] p53-deficient cells also lose p53-mediated cell cycle checkpoints, but retain the S/G2 checkpoints, which was recently shown to be controlled by ATR. ATR stops cells from entering the G2 phase until their replication is complete, by preventing FOXM1 phosphorylation, and its inhibition precipitates replication-defective cells into mitotic catastrophe.[12,13] By abrogating control of the cell cycle checkpoint, loss of p53 may offer a vulnerability to the inhibition of ATR, which plays a central role in orchestrating the molecular response to replication stress.[14] Targeting replication stress in cancer using ATR, CHK1, or WEE1 inhibitors is under clinical evaluation, with or without chemotherapy, or targeted therapies interfering with nucleotide and DNA synthesis.[15] Among them, CTP synthase 1 (CTPS1) inhibitors appear to be of particular interest in cancers of lymphoid origin. Indeed, CTPS1, which is a rate-limiting step enzyme in de novo CTP synthesis, is mainly expressed in lymphoid cells, is involved in activation-induced lymphoid cell proliferation, and is overexpressed in tumor cells of lymphoid origin.[16–18] Of note, in mantle cell lymphoma, *CTPS1* expression was shown to inversely correlate to patient survival.[19] Although CTPS1 and its homolog CTPS2 catalyze the CTP de novo synthesis, only CTPS1 is necessary for the maintenance and growth of lymphoid T and B cells.[18,20] Recently, STP-B, a molecule that selectively targets CTPS1 and which was initially developed to inhibit lymphocyte proliferation in immune disorders, has recently shown significant efficacy in vitro in both lymphoma and myeloma cell lines.[18,21,22] A compound from the same chemical series is currently being evaluated in a clinical trial (NCT05463263).

In this article, we have evaluated the therapeutic potential of STP-B-mediated CTPS1 targeting in *TP53*-deficient myeloma cells in combination with ATR inhibition, in vitro in $TP53^{+/+}/TP53^{-/-}/TP53^{mut}$ CRISPR/Cas9 isogenic myeloma cell lines, ex vivo in del17p patient samples, and in vivo in $TP53^{-/-}$ myeloma xenografted mice.

MATERIALS AND METHODS

Human myeloma cell lines and patient samples

Samples from MM patients were obtained at the University Hospital (MYRACLE cohort, NTC03807128).[23] The isolation of mononuclear cells, purification of myeloma cells, and assessment of del17p status by fluorescence in situ hybridization, as well as the characterization of human myeloma cell lines (HMCLs), have all been reported previously.[24,25] Routine authentication of HMCLs was carried out using a flow cytometry process that has been previously reported.[26] Interleukin-6-dependent and -independent myeloma cells were cultured in RPMI-1640 with 5% foetal calf serum supplemented or not with 3 ng/mL IL-6.

Generation of $TP53^{-/-}$ and $TP53^{R175H/R175H}$ HMCLs

For NCI-H929 and XG7 cell lines, $TP53^{-/-}$ clones were obtained by CRISPR/Cas9 as previously described using two lentiviruses that contain Cas9 or an inducible single-guide RNA (sgRNA) directed against the *TP53* codons 157 and 158, after transient culture with 10 µM Nutlin3a to kill unmodified $TP53^{+/+}$ cells, prior to cloning by limiting dilution.[27] Control $TP53^{+/+}$ clones (n = 3) were obtained from noninduced infected cells after limiting dilution. $TP53^{R175H/R175H}$ XG7 clones (n = 3) were obtained through homologous recombination following the manufacturer's instructions (Integrated DNA Technologies [IDT]): 500,000 cells were transiently electroporated

(Nucleofector II) in the presence of Cas9 electroporation enhancer (IDT), with an RNP complex, that is, 18 pmol Cas9 nuclease pre-incubated with 22 pmol AATO550-conjugated tracerRNA and 22 pmol *TP53* specifically methylated sgRNA (5′-mAmGmCAC AATGACGGAGGTTGTG-3′), and a DNA donor containing the R175H (A) and silent mutations (CCC) in codons 173 and 174 in order to prevent additional cleavage (5′-CATGGCCATCTACAAGCAGTC ACAGCACATGACGGAGGTTGTCCGCCACTGCCCCCACCATGAGCG CTGCTCAGATAGCGATGGTGAG-3′). After electroporation, cells were cultured in complete medium in the presence of 1 µM HDR enhancer V2 to prevent NHEJ recombination during 24 h (IDT). After 3 days, cells were transiently cultured for 2 days with 10 µM Nutlin3a to kill $TP53^{+/+}$ unmodified XG7 cells prior to cloning by limiting dilution. Clones were characterized for *TP53* sequence and overexpression of p53 protein to select three independent clones harboring the *R175H* mutation.

Reagents and antibodies

STP-B was provided by Step Pharma.[28,29] The pan-caspase inhibitor Q-VD-OPh, NAC (*N*-acetyl cysteine), and the ATR inhibitors VE-821 and AZD6738 were purchased from Sigma-Aldrich or MedChemExpress. Anti-CD138-PE monoclonal antibody (mAb) came from Beckman Coulter, Annexin-V-APC from Immunotools, anti-BrdU-AF647 mAb from BD Pharmingen, and γ-H2AX-AF647 and antipuromycin mAb from Millipore.

Cell death assays

Myeloma cells were treated with STP-B (1–10,000 nM) alone or in combination with VE-821 (1.25–5 µM) for 24–72 h. Cell viability was assessed by CellTiter-Glo assay. Cell death was assessed using Annexin-V staining (HMCLs) or loss of CD138 staining (patient samples) with flow cytometry.[10,24]

Transcriptomic analysis

Genomic profiling of HMCLs, clones, or patient samples (MYRACLE) was determined by 3′ Seq RNA profiling (SRP), as described previously.[27] Single-cell RNA-sequencing (scRNA-seq) analysis of patient samples has been previously described (EGA50000000044).[27] Expression profiling analysis was carried out on 684 patient samples from the MMRF-CoMMpass cohort (https://themmrf.org) and 139 patients in the CASSIOPEA clinical trial.[30]

Functional p53 score

A functional 8-gene p53 score, based on the ranked expression of eight p53-target genes, that is, *APOBEC3H*, *BAX*, *CDKN1A*, *DDB2*, *EDA2R*, *MDM2*, *PHLDA3*, and *RPS27L*, was calculated using the rank-based gene set scoring method with the singscore package in R, as previously described, with minor adaptations (the 8-gene score was adapted from the 13-gene score).[27,31]

MM xenograft model

NCI-H929 $TP53^{-/-}$ cells were engrafted subcutaneously in NOD-scid IL2Rgamma (NSG) mice (1 × 10⁶ cells/mouse). After 1 week, mice with a tumor volume of 100 mm³ were randomly distributed into four groups of seven mice that were treated, or not treated, with STP-B

(30 mg/kg) injected subcutaneously and/or with AZD6738 (25 mg/kg) delivered by oral gavage. STP-B was formulated in 10% benzyl alcohol and 90% castor oil, while AZD6738 was prepared in 10% DMSO, 40% PEG300, 5% Tween-80, and 45% saline solution.

Statistical analysis

Statistical analyses were carried out using the nonparametric Mann–Whitney, Kruskal–Wallis, Friedman, and the parametric two-way analysis of variance tests, as indicated in the legends of the figures. Survival analyses were carried out using the log-rank (Mantel–Cox) test. Statistical significance is indicated in the figures with symbols $*p < 0.05$, $**p < 0.01$, $***p < 0.001$, and $****p < 0.0001$.

RESULTS

Increased *CTPS1* expression is associated with proliferation and *TP53* deficiency in myeloma cells

CTPS1 and *CTPS2* expression was analyzed in 684 MM patients from the MMRF-CoMMpass cohort, characterized for both del17p and *TP53* mutation, and in 139 patients from the CASSIOPEA clinical trial including 137 characterized for del17p.[27] In MMRF-CoMMpass patients, *CTPS1*, and not *CTPS2*, expression was significantly higher in 58 of the samples with *TP53* hits, that is, del17p ($n = 34$), del17p and *TP53* mutation ($n = 19$), or *TP53* mutation ($n = 5$), compared to 626 samples without ($p = 0.0007$ and $p = 0.3$, respectively; Figure 1A). Similarly, in CASSIOPEA patients, *CTPS1*, and not *CTPS2*, expression was significantly higher in 12 samples with del17p versus 125 without ($p = 0.0039$ and $p = 0.83$, respectively; Figure 1A). To determine whether high *CTPS1* expression in the *TP53*abnormal cells was related to p53 or to proliferation, we analyzed the expression of *MKI67* and *CCNB1* and used a functional score to reflect p53 transcriptomic activity (p53 score). In both cohorts, *MKI67* ($p < 0.0001$ and $p = 0.0006$ in MMRF-CoMMpass and CASSIOPEA, respectively) and *CCNB1* ($p < 0.0001$ and $p = 0.0006$ in MMRF-CoMMpass and CASSIOPEA, respectively) expression was higher in *TP53*abn samples compared to *TP53*wt samples (Figure 1A). *CTPS1* and *MKI67* expression correlated in both cohorts independently of *TP53* status (Figure 1B, upper panels). Using a functional 8-gene p53 score derived from the 13-gene score we previously reported (Figure S1),[27] we further evaluated whether *CTPS1* expression could reflect p53 activity: indeed, *CTPS1* expression and the p53 score showed significant correlation in samples from patients in MMRF-CoMMpass and CASSIOPEA ($p < 0.0001$ and $p = 0.007$, respectively), and the correlation was restricted to samples with a normal *TP53* status (Figure 1B, middle panels). Interestingly, the p53 score and *MKI67* expression positively correlated in the *TP53*wt samples in both cohorts and negatively correlated in the *TP53*abn samples in MMRF-CoMMpass (the weak del17p number in CASSIOPEA excluded definitive analysis; Figure 1B, lower panel). These results might suggest that a high p53 score in *TP53*wt samples reflects a high proliferation rate, while a low p53 score in *TP53*abn samples reflects low p53 transcriptomic activity despite the high proliferation rate. Taken together, these results showed that samples with high proliferation rates and/or abnormal *TP53* status displayed high *CTPS1* expression.

Lastly, to confirm this direct association between *CTPS1* expression and proliferation in myeloma samples, we used scRNA-seq technology. Myeloma cells ($n = 55,114$) were identified within 23 mononuclear bone marrow samples, and one pleural effusion sample, as reported previously (Figure S2).[27] Expression of *CTPS1*, *MKI67*, and

CTPS2 was analyzed in 40,266, 11,936, and 2912 myeloma cells in G1, S, and G2/M phase, respectively (Figure 2A): *CTPS1*, but not *CTPS2*, was expressed throughout the cell cycle, with maximum expression in the S and G2/M phases (Figure 2B).

As expected, the patients with a high expression of *MKI67* or *CTPS1*, and not of *CTPS2*, had significantly reduced survival in both cohorts, and multivariate Cox analysis showed that *CTPS1* expression retained significance, independently from proliferation (Figure S3). Collectively, these results show that *CTPS1* was highly expressed in proliferating MM cells, particularly in cells with *TP53* hits, and that high *CTPS1* levels were associated with poor outcomes, justifying its selective targeting in p53-deficient cells.

### *TP53* status had no impact on *CTPS1* expression in cell lines

To confirm that *CTPS1* expression is not under the direct control of p53, in contrast to *BAX* expression, we analyzed *CTPS1* and *CTPS2* expression in 16 HMCLs and in 15 isogenic *TP53*+/+, *TP53*−/−, and *TP53*R175H/R175H clones (Figure S4), using differential gene expression sequencing (DGE-seq), as previously reported.[27] As shown in Figure 3A,B, *CTPS1* was significantly expressed at higher levels than *CTPS2* in both HMCLs and isogenic clones ($p ≤ 0.001$), and *TP53* status did not significantly impact the constitutive *CTPS1* expression (the under expression of *CTPS2* in two *TP53*−/− and eight *TP53*−/mut HMCLs was not confirmed in the NCI-H929 or XG7 *TP53* isogenic clones, excluding the direct impact of p53 on *CTPS2* expression). To assess the direct regulation by p53, we used Nutlin3a, an MDM2 inhibitor that prevents p53 degradation and, therefore, increases p53 expression. We showed that *CTPS1* or *CTPS2* expression was not regulated upon the activation of the p53 pathway, in contrast to *BAX*, a well-known target of p53, whose expression was increased by Nutlin3a in a p53-dependent manner (Figure 3B, lower panels). These results clearly confirmed that p53 did not directly control the expression of *CTPS1* and *CTPS2*.

To assess the efficacy of targeting CTPS1 in *TP53*-deficient myeloma cells, we used STP-B, a selective inhibitor of CTPS1.[28] Treatment with STP-B for 72 h resulted in a loss of CTG incorporation in all HMCLs tested (median $IC_{50} = 500$ nM), irrespective of p53 status (wild type, deleted, and mutated) (Figure 3C and Table 1). There was no significant difference in STP-B IC_{50} values between *TP53*+/+ and *TP53*−/− or *TP53*R175H/R175H clones from NCI-H929 or XG7 ($p = 0.21$; Figure 3D and Table 1), although *TP53*−/− clones from NCI-H929 appeared less sensitive to a high STP-B concentration ($≥300$ nM) than the control clones. These results showed that *CTPS1* expression is independent of *TP53* status in cell lines and that CTPS1 inhibition efficiently reduces the viability of p53-deficient myeloma cells.

CTPS1 inhibitor STP-B induced early S-phase cell cycle arrest in p53-proficient and p53-deficient cells

To characterize the functional consequences of selective CTPS1 inhibition in myeloma cells, transcriptomic analysis was carried out using SRP in 10 HMCLs selected to represent myeloma genomic heterogeneity and different *TP53* statuses (Table 1). Following STP-B treatment (STP-B IC_{50} for 24 h), 11 genes were upregulated in STP-B-treated cells, and 31 were downregulated (false discovery rate <0.05; Figure 4A). Using the Reactome database, the functional annotation of the transcriptomic response to STP-B in 10 HMCLs identified a significant decrease in the G2/M-phase signature (*PLK1*, *CCNB1*, *CDC20*, and *CEP63*) and in the protein translation signature (*RPL22*,
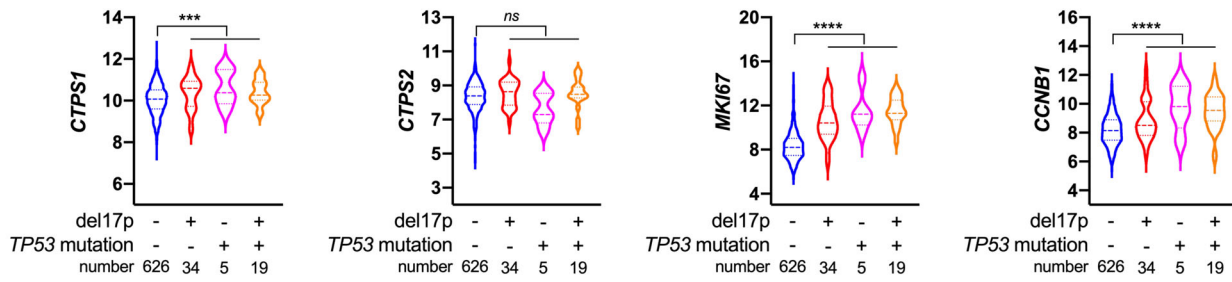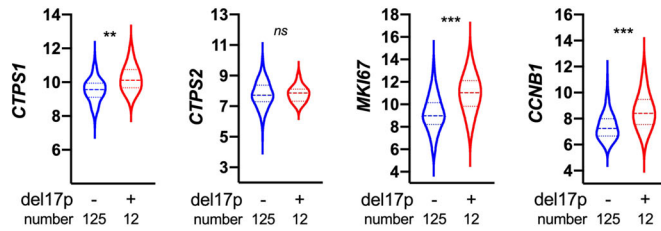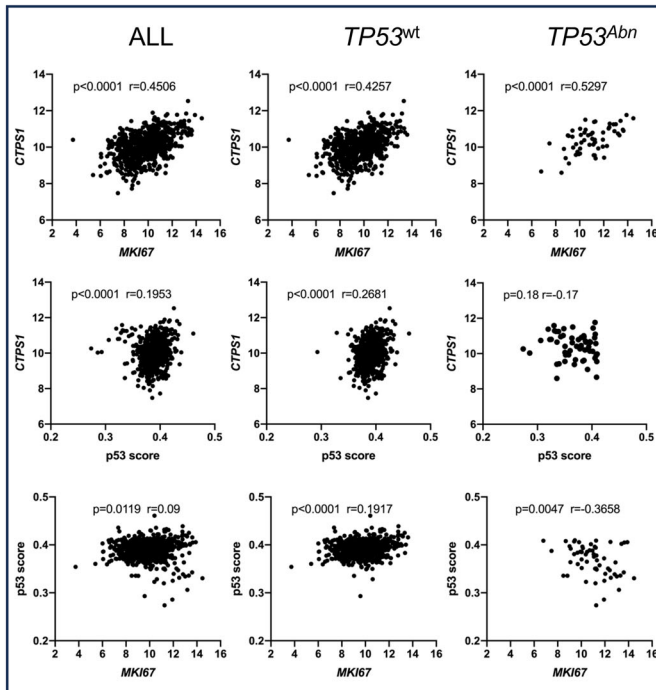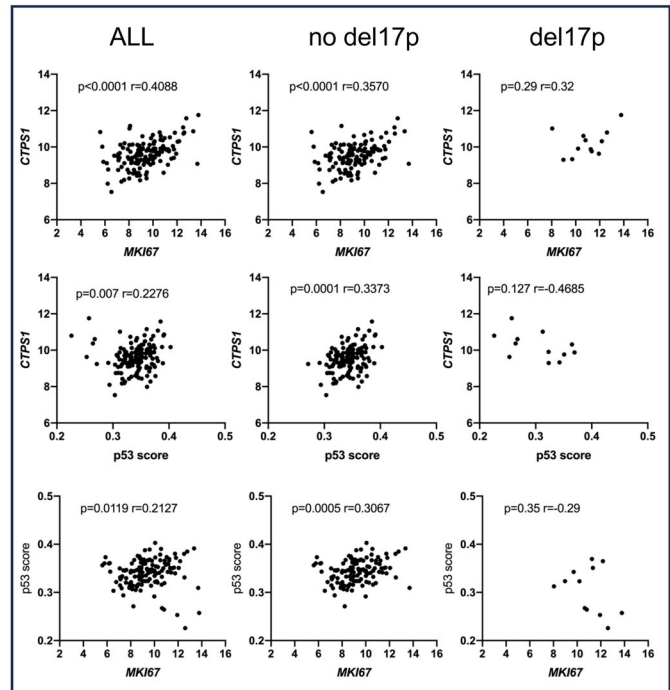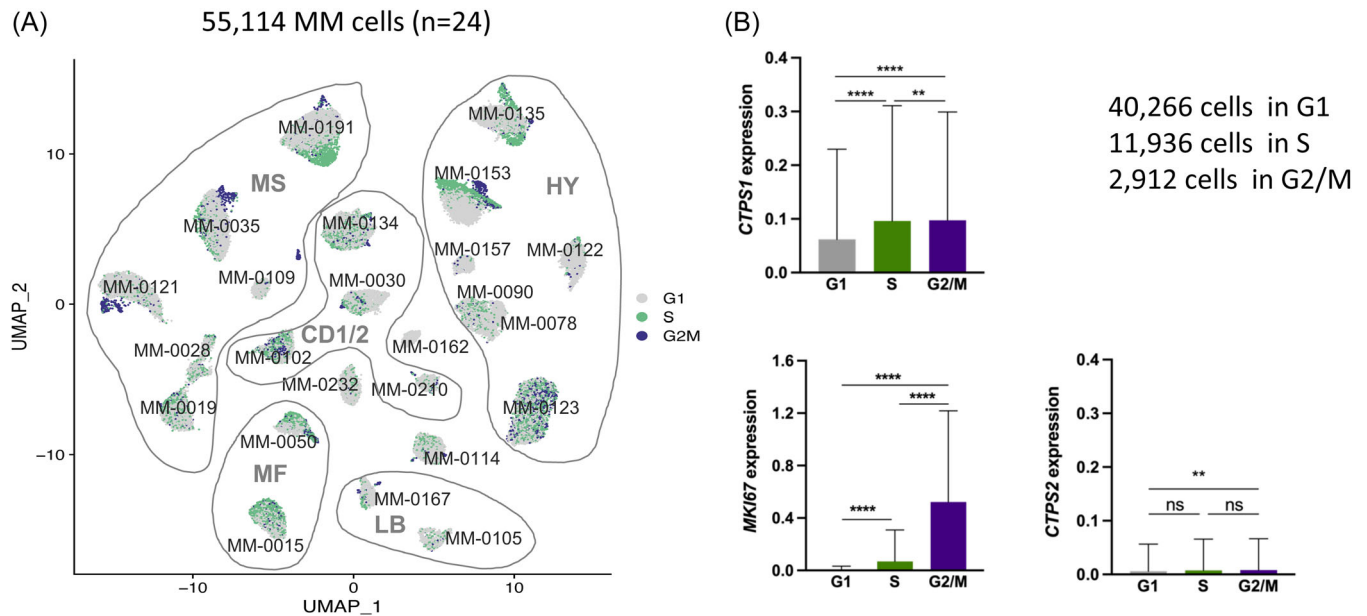
FIGURE 1 **CTP synthase 1 (CTPS1) expression is associated with proliferation and is increased in TP53abnormal myeloma cells. (A)** TP53abnormal myeloma cells overexpress *CTPS1*, *MKI67*, and *CCNB1*. Upper panel: Expression of *CTPS1*, *CTPS2*, *MKI67*, and *CCNB1* was assessed by RNA-seq in myeloma cells from 684 patients (MMRF-CoMMpass) annotated for *TP53* status (*TP53* deletion and/or *TP53* mutation). *TP53* status was considered abnormal when a VAF was inferior to −0.5 (deletion) or superior to 0.3 (mutation). Lower panel: Expression of *CTPS1*, *CTPS2*, *MKI67*, and *CCNB1* was assessed by RNA-seq in 137 myeloma samples (CASSIOPEIA) annotated for del17p. Del17p was considered positive when 50% of myeloma cells displayed 17p deletion. Statistical significance was determined using the Mann–Whitney test. **(B)** *CTPS1* expression correlates with *MKI67* expression or p53 score in patient samples. The expression of *CTPS1* in the MMRF-coMMpass or CASSIOPEIA cohort was analyzed according to *MKI67* expression (upper panels), p53 score (middle panels) in all, *TP53*wt, *TP53*abn MMRF-coMMpass samples or in all, del17p, and no del17p samples in CASSIOPEIA, respectively. Correlation between p53 score and *MKI67* expression was assessed in all *TP53*wt, *TP53*abn MMRF-coMMpass samples or in all del17p, no del17p samples in CASSIOPEIA, respectively (lower panels). Statistical significance was determined using Spearman's test. Statistical significance is indicated in the figures with symbols **p < 0.01, ***p < 0.001 and ****p < 0.0001. ns, Not significant.

(A)

55,114 MM cells (n=24)

(B)

40,266 cells in G1
11,936 cells in S
2,912 cells in G2/M

FIGURE 2 Myeloma cells in S and G2M phases overexpress CTP synthase 1 (*CTPS1*). (A) Myeloma cells in S and G2/M phases overexpress *CTPS1* and not *CTPS2*. UMAP (uniform manifold approximation and projection) representation of myeloma cells from 24 samples (23 bone marrow and one pleural effusion).[27] The myeloma classification of samples is indicated (MS, CD-1/2, MF, LB, and HY). Mononuclear cells from the bone marrow or pleural effusion (MM-0191) of 24 multiple myeloma patients were cultured overnight in RPMI-1640 with 10% fetal calf serum and 3 ng/mL interleukin-6 before undergoing cell processing and single-cell RNA-sequencing analysis. Myeloma cells were identified as described previously.[27] Cell cycle signature was calculated using the AddModuleScore function of the Seurat package in R (gray: G1 phase; green: S phase; purple: G2/M phase). (B) The graphs represent the mean ± SD of *CTPS1*, *MKI67*, and *CTPS2* expression in 55,114 myeloma cells according to the cell cycle phase. Statistical significance was determined using the Kruskal–Wallis test with Dunn's multiple comparison test. Statistical significance is indicated in the figures with symbols **$p < 0.01$ and ****$p < 0.0001$. ns, Not significant.

RPL23, *RPL27*, and *RPS3A*; Figure 4A,B). To further analyze the functional impact of CTPS1 inhibition on the cell cycle, NCI-H929 and XG7 clones, as well as *TP53*$^{-/-R213STOP}$ myeloma cells from a patient with plasma cell leukemia (PCL#1), were incubated for 24 h with STP-B, before bromodeoxyuridine (BrdU)/propidium iodide staining. As illustrated in Figure 4C and summarized in Figure 4D, STP-B induced a significant accumulation of cells blocked in the early S phase in *TP53*$^{+/+}$, *TP53*$^{-/-}$, and *TP53*$^{R175H/R175H}$ clones, as well as in *TP53*$^{-/R213STOP}$ PCL#1 (mean increase 2.3-fold, $p = 0.001$). The accumulation in the early S phase was associated with a consequent decrease in G1, late S, and G2/M phases (mean decrease 1.7-, 1.3-, and 3.1-fold, respectively, $p = 0.001$). Taken together, these results suggest that CTP depletion resulting from CTPS1 inhibition induced early S-phase arrest, irrespective of *TP53* status.

Simultaneous CTPS1 and ATR targeting showed synergistic efficacy in *TP53*-deficient myeloma cells

As STP-B efficiently induced S-phase arrest in p53-deficient cells, we thought about inhibiting ATR, the S/G2 cell cycle checkpoint, so as to induce mitotic catastrophe and cell death.[12] ATR is of particular interest in MM as it is rarely deleted or mutated, and myeloma cells have been shown to be addicted to ATR.[32,33] Transcriptomic analysis showed that *TP53* status did not impact *ATR* expression in HMCLs, isogenic myeloma clones, or patient samples (Figure 5A–C). Single-cell analysis further showed that *ATR* was well-expressed irrespective of cell cycle phase cells (Figure 5D). We next used VE-821, a selective ATP-competitive inhibitor of ATR, which has minimal activity against ATM, to assess the efficacy in combination with STP-B.[33] Indeed, 200 nM STP-B with 2.5 μM VE-821 induced 37.5% and 53.5% cell

death in four *TP53*^{wt} and five *TP53*^{abnormal} HMCLs, respectively ($p = 0.9$; Figure 6A, left panel). The efficacy of the combination was similar in NCI-H929 and XG7 clones, irrespective of *TP53* status, although it was slightly less effective in *TP53*$^{R175H/R175H}$ compared to *TP53*$^{+/+}$ XG7 clones (mean death was 55% versus 64%, respectively; Figure 6A, middle and right panels).

The STP-B/VE-821 combination proved highly synergistic, as shown by the Bliss scores, which were above 15 for all the clones (Figure 6B). The strong cytotoxicity of the combination was associated with γ-H2AX staining, indicating an increase in DNA strand breaks, a hallmark of mitotic catastrophe (Figure 6C).

Simultaneous targeting of CTPS1 and ATR induced a caspase-dependent dell death and disrupted protein translation

To further characterize cell death induced by STP-B and VE-821, we first assessed whether cell death was strictly related to CTPS activity by complementing the culture medium with CTP to counteract inhibition of the de novo CTP synthesis induced by STP-B.[21] Indeed, daily addition of 200 μM of CTP highly prevented cell death induced by STP-B alone or in combination with ATR (Figure 7A): taking all *TP53*$^{+/+}$, *TP53*$^{-/-}$ NCI-H929 and XG7 clones together, the mean inhibition of cell death induced by STP-B alone or in combination with VE-821 was 102.4% ± 7.5% and 92.6% ± 14.4%, respectively.

We next determined the involvement of caspase or ROS in cell death by using a caspase inhibitor or an ROS scavenger, the impact on protein translation by measuring puromycin incorporation, and the induction of replicative stress by assessing CHK1 and CHK2 phosphorylation.
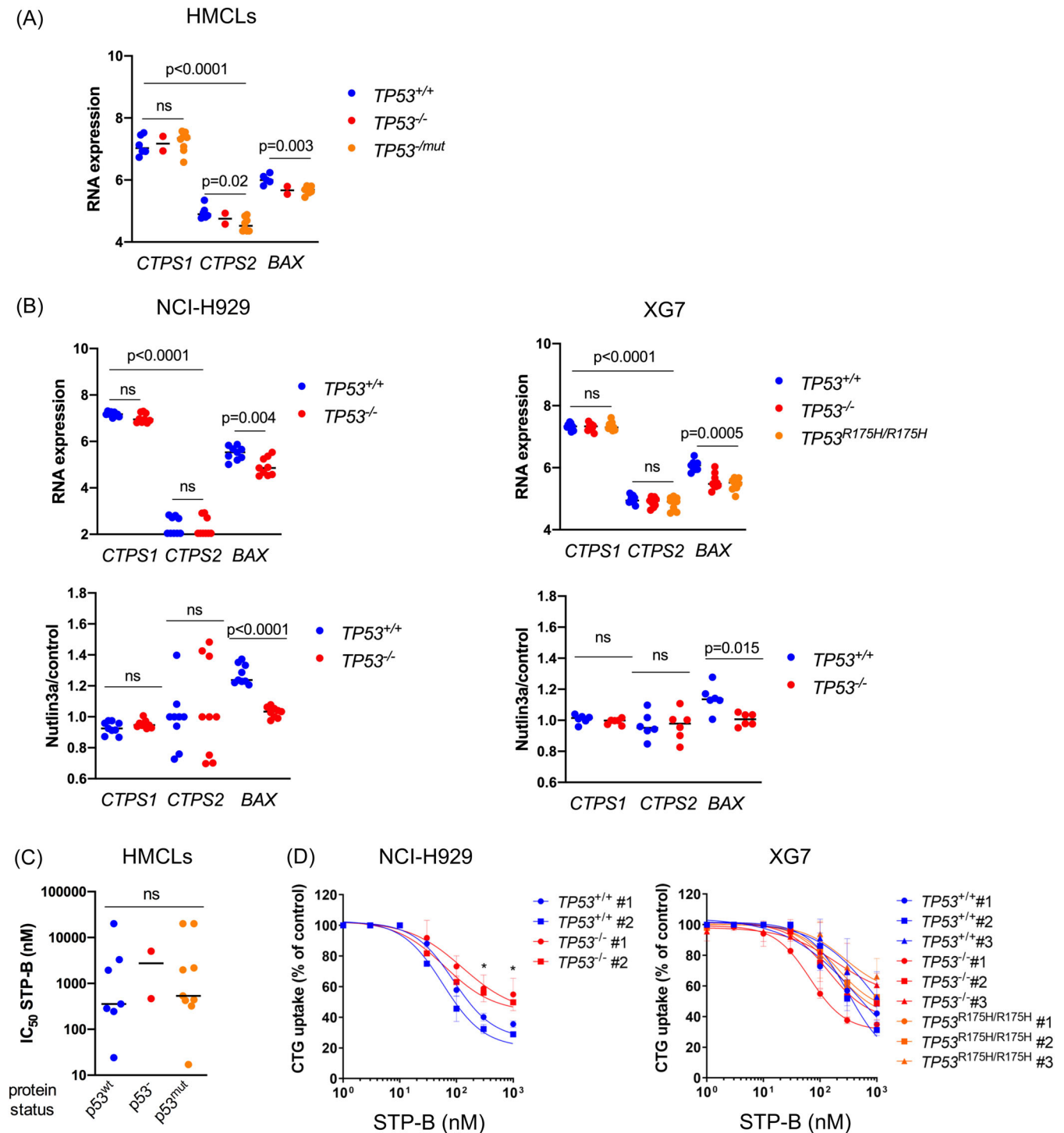
FIGURE 3 CTP synthase 1 (*CTPS1*) expression and response to CTPS1 inhibitor are not regulated by p53. **(A)** *CTPS1*, and not *CTPS2*, is highly expressed in *TP53*[abnormal] myeloma cells. *CTPS1*, *CTPS2*, and *BAX* expression was assessed by SRP in 16 human myeloma cell lines (HMCLs). Statistical significance was determined using the Kruskal–Wallis and Mann–Whitney tests. **(B)** The expression of *CTPS1* and CTPS2 is not regulated by p53. Upper panel: *CTPS1*, *CTPS2*, and *BAX* expression was assessed using SRP in the six isogenic NCI-H929 clones (three *TP53*^{+/+} and three *TP53*^{−/−} clones), as well as in the nine XG7 clones (three *TP53*^{+/+}, three *TP53*^{−/−}, and three *TP53*[R175H/R175H]). Statistical significance was determined using the Kruskal–Wallis test. Lower panel: *CTPS1*, *CTPS2*, and *BAX* expression was assessed using SRP in the NCI-H929 and XG7 clones treated, or not, with Nutlin3a (10 μM in NCI-H929 and 2 μM in XG7) for 18 h. Results are expressed as the fold expression in Nutlin3a-treated cells over untreated cells. Statistical significance was determined using the Kruskal–Wallis and Mann–Whitney tests. **(C, D)** *TP53*[abnormal] myeloma cells are sensitive to CTPS1 inhibitor STP-B. Response to STP-B was assessed by CellTiter-Glo assay after 72 h of culture in **(C)** 18 HMCLs and in **(D)** *TP53* isogenic clones from NCI-H929 or XG7, as indicated. STP-B half-maximal inhibitory concentration (IC$_{50}$) values were compared in HMCLs according to their p53 protein status. STP-B IC$_{50}$ values of HMCLs and clones are detailed in Table 1. Results represent the mean of two to three independent experiments performed in triplicate. Statistical significance was determined using the Kruskal–Wallis and Mann–Whitney tests. ns, Not significant.

TABLE 1 STP-B IC$_{50}$ values in HMCLs and isogenic clones.

| HMCLs	TP53 sequence	p53 WB	Cytogenetic group	STP-B IC$_{50}$ (nM)
TP53^{wt}				
AMO1	+/+	+ (53 kDa)	OTHER	285
MDN	+/+	+ (53 kDa)	CCND1	24
MM1S	+/+	+ (53 kDa)	MAF	3287
NAN11	+/−	+ (53 kDa)	MAF	>10,000
NCI-H929	+/+	+ (53 kDa)	MS	245
XG6	+/+	+ (53 kDa)	MAF	1937
XG7	+/+	+ (53 kDa)	MS	356
TP53Abn				
JIM3	R273C/−	+ (53 kDa)	MS	2181
JJN3	−/−	-	MAF	ND
KMM1	C135F/S241F	+ (53 kDa)	OTHER	424
KMS12PE	R337L/−	+ (53 kDa)	CCND1	>10,000
L363	S261T/−	+/− (53 kDa)	MAF	440
LP1	E286K/−	+ (53 kDa)	MS	ND
NAN1	E180STOP/−	-	MAF	5031
NAN3	R248Q/−	+ (53 kDa)	MS	1966
NAN6	Del exons 7–9/−	+ (35 kDa)	MAF	322
NAN8	D21Y/−	-	MS	466
OPM2	R175H/−	+ (53 kDa)	MS	ND
U266	A161T/−	+ (53 kDa)	CCND1	ND
XG2	C176Y/R213STOP	+ (53 kDa)	OTHER	533
XG5	R282W/−	+ (53 kDa)	CCND1	>10,000
XG11	C135Y/−	+ (53 kDa)	CCND1	17
TP53 clones				
NCI-H929 *TP53*$^{+/+}$ #1	+/+	+ (53 kDa)	MS	165
NCI-H929 *TP53*$^{+/+}$ #2	+/+	+ (53 kDa)	MS	93
NCI-H929 *TP53*$^{−/−}$ #1	−/−	-	MS	1043
NCI-H929 *TP53*$^{−/−}$ #2	−/−	-	MS	486
XG7 *TP53*$^{+/+}$ #1	+/+	+ (53 kDa)	MS	552
XG7 *TP53*$^{+/+}$ #2	+/+	+ (53 kDa)	MS	379
XG7 *TP53*$^{+/+}$ #3	+/+	+ (53 kDa)	MS	1108
XG7 *TP53*$^{−/−}$ #1	−/−	-	MS	129
XG7 *TP53*$^{−/−}$ #2	−/−	-	MS	453
XG7 *TP53*$^{−/−}$ #3	−/−	-	MS	>10,000
XG7 *TP53*$^{R175H/R175H}$ #1	R175H/R175H	+ (53 kDa)	MS	661
XG7 *TP53*$^{R175H/R175H}$ #2	R175H/R175H	+ (53 kDa)	MS	991
XG7 *TP53*$^{R175H/R175H}$ #3	R175H/R175H	+ (53 kDa)	MS	>10,000

Note: STP-B IC$_{50}$ value in 18 HMCLs and 13 *TP53* isogenic clones from NCI-H929 and XG7 was determined using a 72-h CellTiter-Glo assay. *TP53* status (mutation and/or deletion), cytogenetic group, and p53 status are indicated.

Abbreviations: HMCL, human myeloma cell line; IC$_{50}$, half-maximal inhibitory concentration; ND, not determined; WB, western blot.

The addition of the pan-caspase inhibitor Q-VD inhibited cell death induced by STP-B alone or in combination with VE-821 by about 50% in five HMCLs or clones tested: STP-B-induced cell death was 8% ± 2% versus 20% ± 5% in Q-VD versus control, $p = 0.06$, and STP-B+VE-821-induced cell death was 25.5% ± 2.5% versus 53% ± 6% in Q-VD versus control, $p = 0.0051$, respectively, indicating the involvement of caspase in cell death in the five HMCLs or clones tested (Figure 7B, left panel). In contrast, the addition of 5 mM NAC did not inhibit cell death, excluding the involvement of ROS (Figure 7B, middle panel).
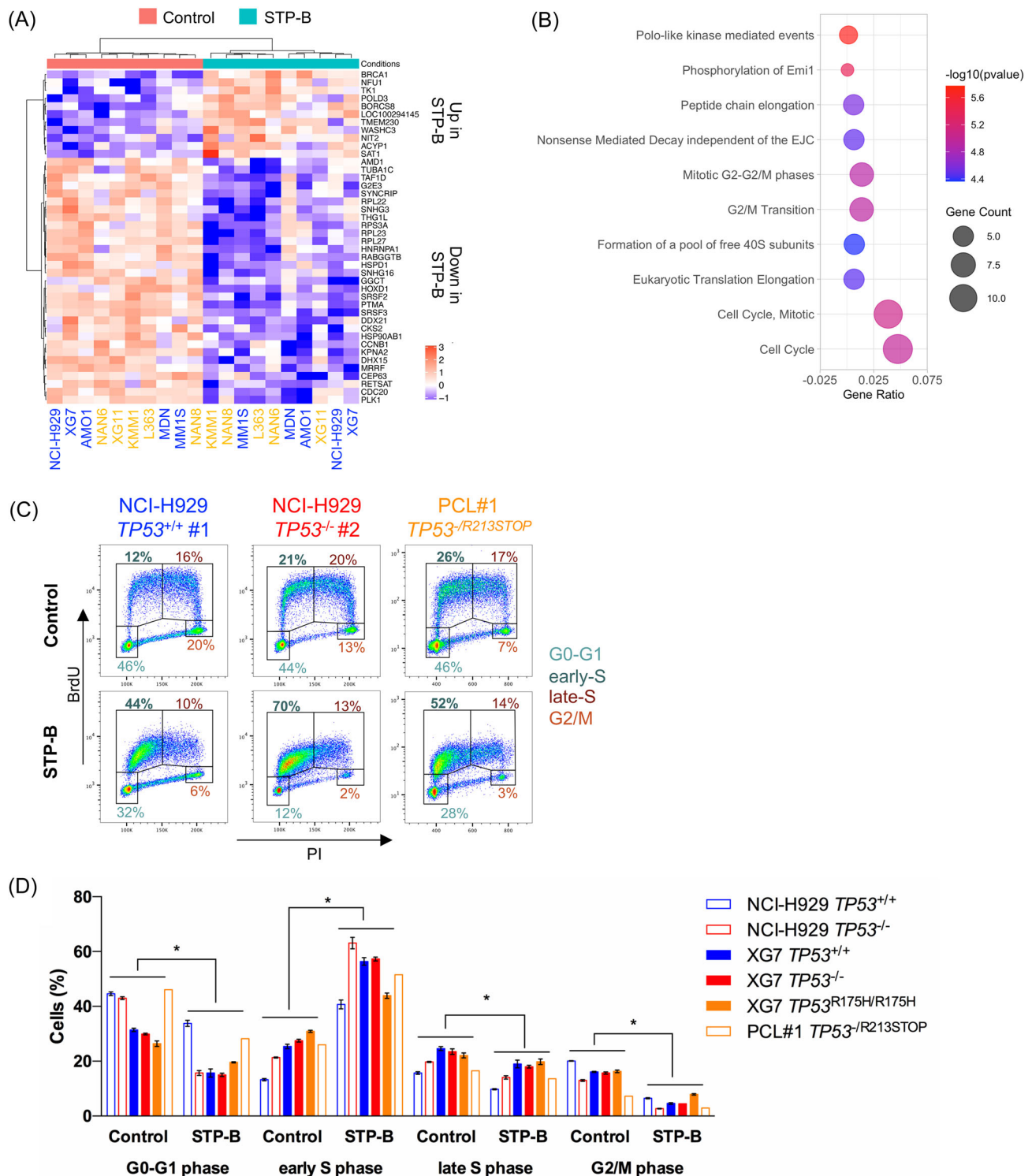
FIGURE 4 STP-B induces early S-phase cell cycle arrest in myeloma cells regardless of their *TP53* status. **(A)** STP-B modulates the expression of 42 genes in myeloma cell lines Transcriptomic profiling was performed using SRP in 10 human myeloma cell lines (HMCLs) (five *TP53*wt HMCLs annotated in blue and five *TP53*abnormal HMCLs in yellow; see Table 1). HMCLs were treated for 24 h with STP-B IC$_{50}$ before RNA extraction and sequencing. Genes with significant differential expression (log 2 fold change <−0.5 or >0.5 and adjusted *p* < 0.05) were selected and shown in the supervised hierarchical clustering (control vs. STP-B). **(B)** CTPS1 inhibition affects transcriptional programs related to cell cycle and translation. Pathway enrichment analysis was conducted using Reactome. The graph represents the 10 pathways most significantly affected by STP-B treatment. **(C, D)** STP-B induces early S-phase cell cycle arrest in *TP53*abnormal clones and in a patient sample. Cells were treated for 24 h with 200 nM STP-B before incubation with bromodeoxyuridine (BrdU) from 30 (clones) to 90 min (patient sample). Cells were then fixed, permeabilized, stained with anti-BrdU antibody and propidium iodide (PI), and analyzed using flow cytometry. **(C)** Representative BrdU/PI profiles of two NCI-H929 clones (*TP53*+/+ #1 and *TP53*−/− #2) and of myeloma cells derived from a patient with plasma cell leukemia (PCL) with an abnormal *TP53* status (PCL#1 *TP53*−/R213STOP). **(D)** The bar graph summarizes the percentage of cells in G1, early S, late S, and G2/M phases in *TP53* isogenic clones from NCI-H929 and XG7 and in the PCL#1 patient sample treated or not with STP-B. Statistical significance was determined using the Wilcoxon test. Statistical significance is indicated in the figures with symbol *p < 0.05.
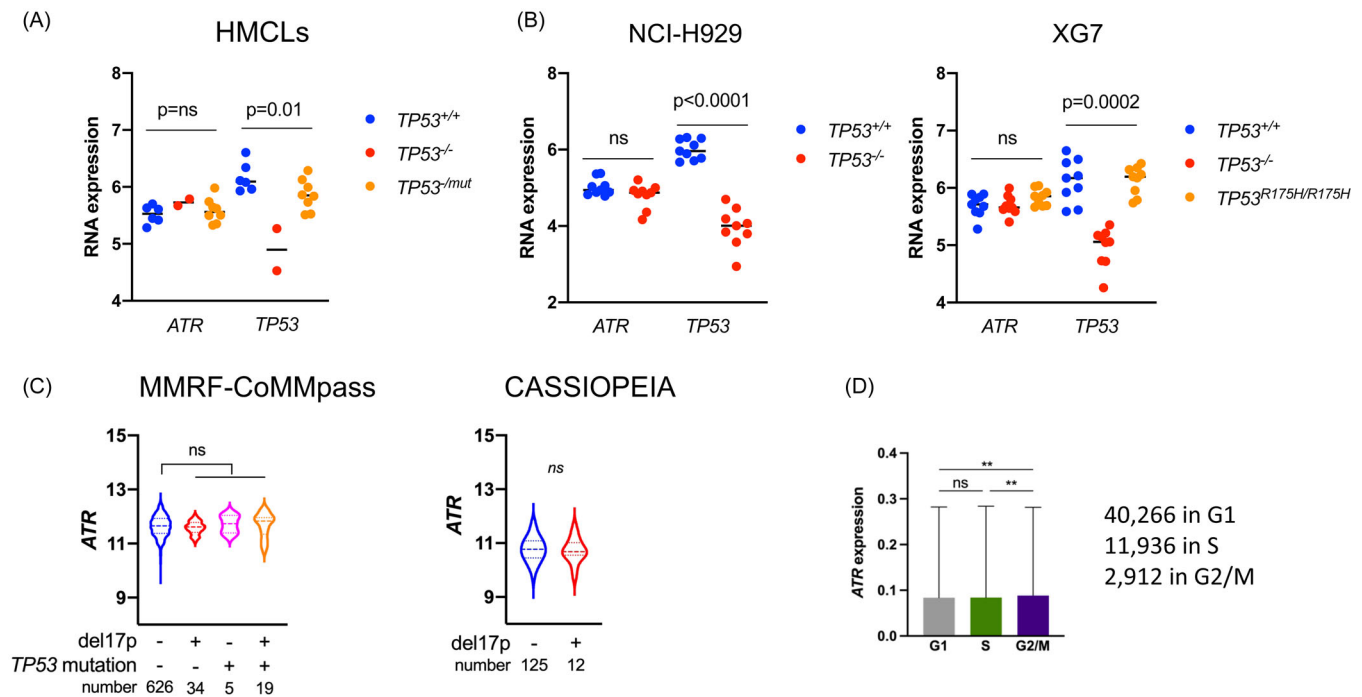
FIGURE 5 *ATR* is expressed in multiple myeloma (MM) cells irrespective of *TP53* status and cell cycle. **(A)** *ATR* expression was analyzed in $TP53^{+/+}$, $TP53^{-/-}$, or $TP53^{-/mut}$ human myeloma cell lines using SRP. **(B)** *ATR* expression was analyzed in $TP53^{+/+}$, $TP53^{-/-}$, or $TP53^{R175H/R175H}$ XG7 and/or NCI-H929 clones using SRP 8B. **(C)** *ATR* expression was analyzed according to the presence of del17p and/or *TP53* mutation in the MMRF-CoMMpass cohort and according to the presence of del17p in the CASSIOPEIA cohort. **(D)** *ATR* expression in the 55,114 MM cells (see Figure 2) according to the cell cycle phase (mean ± SD). Statistical significance was determined using the Kruskal–Wallis test with Dunn's multiple comparison test. Statistical significance is indicated in the figures with symbol **p < 0.01. ns, Not significant.

As expected, puromycin incorporation in $TP53^{+/+}$ or $TP53^{-/-}$ NCI-H929 cells was decreased by STP-B, confirming a decrease in protein translation (23% ± 10%) that was not further modified by VE-821 (22% ± 0.09%; Figure 7C).[22] In both $TP53^{+/+}$ and $TP53^{-/-}$ NCI-H929 and XG7 cells, STP-B induced a strong CHK1 phosphorylation that was not inhibited by VE-821 at 24 h. Of note, VE-821 alone or with STP-B induced P-CHK2, suggesting an activation of ATM pathway (Figure 7D).[33]
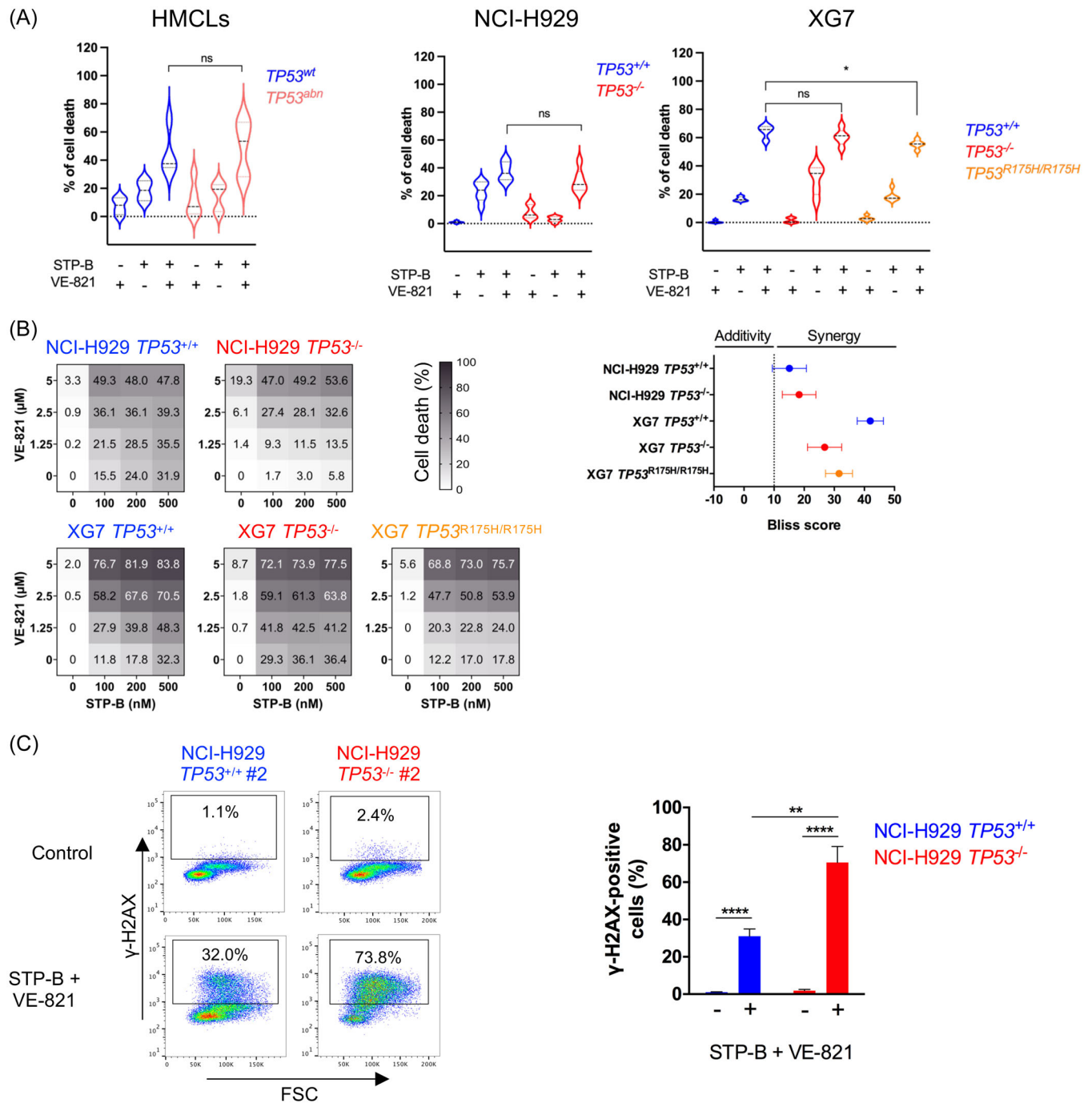
Combined inhibition of CTPS1 and ATR was efficient in p53-deficient cells ex vivo and in vivo

The efficacy of the combination was then assessed, ex vivo, in bone marrow and peripheral blood samples from 17 newly diagnosed (D, n = 5), relapsed (R, n = 6), and resistant/refractory (RR, n = 6) patients. After 72 h of culture with 200 nM STP-B, 2.5 μM VE-821, or a combination of them, median cell death was 2.2% (0–24.9), 12.6% (0–28.7), and 18.3% (0–59.9), respectively (Figure 8A). Cell death induced by the combination was additive to synergistic in 17 samples and highly effective in RR samples (median of cell death was 38.6%; Table 2). In the 15 samples with known del17p status (five with del17p and 10 without), the median death was 42.9% versus 7.45% in samples with del17p compared to those without del17p (p = 0.008) and the combination was synergistic in the five del17p samples (p = 0.02) (Figure 8B). The efficacy of the combination in del17p samples prompted us to assess the efficacy of STP-B and AZD6738 in vivo, with a clinical grade, orally available inhibitor of ATR, using xenografted $TP53^{-/-}$ NCI-H929 NSG mice.[34] The mice were treated over 2 weeks, 5 days a week, and then left untreated for 2 days (Figure 8C), middle panel). Each drug induced a significant delay in

tumor growth as single agents, and their combination was highly effective: between Days 1 and 12, the increase in tumor size was 10.0-, 6.4-, 3.5-fold, and 1.6-fold in control, STP-B, AZD6738, and combo groups, respectively (Figure 8C, middle and right panel). Both single and combined compounds were well-tolerated, with body weight variations of less than 10% (Figure S5).

DISCUSSION

The aim of this study was to determine whether the inhibition of CTPS1, an enzyme critical for CTP synthesis and essential for sustaining DNA synthesis in normal and malignant lymphoid cells, could constitute an actionable vulnerability in *TP53*-deficient myeloma cells.[16–18] *CTPS1* was indeed overexpressed in patient samples with del17p and/or *TP53* mutations, compared to samples without *TP53* hits in two different patient cohorts (MMRF-CoMMpass and CAS-SIOPEIA). *CTPS1* expression correlated with *MKI67* and *CCNB1* expression, both of which were increased in patient samples with del17p and/or *TP53* mutation. The analysis of *CTPS1* and *MKI67* expression and the p53 score values showed that high *CTPS1* expression was synonymous with high *MKI67* expression, which correlated to a p53 score positively in $TP53^{wt}$ myeloma cells and negatively in $TP53^{Abnormal}$ myeloma cells. The association between *CTPS1* expression and proliferation was further confirmed at a single-cell level in 24 patient samples, with *CTPS1* expression being significantly higher in cells in the S and G2/M phases than in the G1 phase. We showed that patients with high *CTPS1* or *MKI67* expression had a shortened survival period in univariate and multivariate analyses. The high *CTPS1* expression in $TP53^{abnnormal}$ samples not only reflects their high proliferation rate but also constitutes a
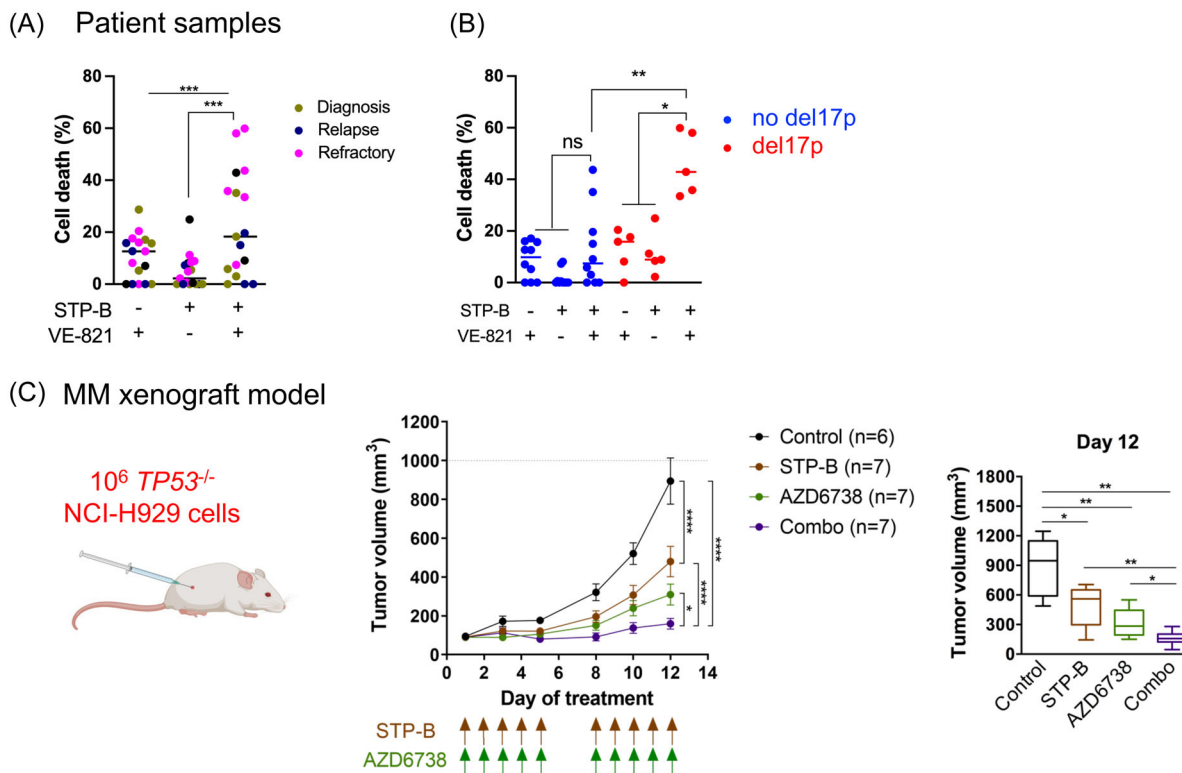
FIGURE 6 The inhibition of CTPS1 and ATR is highly synergistic in p53-deficient myeloma cells in vitro. **(A)** The STP-B and VE-821 combination is efficient in *TP53*abnormal human myeloma cell lines (HMCLs) and in isogenic clones. Left panel: Four *TP53*wt HMCLs (AMO1, BCN, XG6, and XG7) and five *TP53*abnormal HMCLs (Karpas620, KMS12PE, NAN8, U266, and XG11) were treated for 72 h with 200 nM STP-B, 2.5 μM VE-821 or both (except XG11, which was treated with 10 nM STP-B and 1 μM VE-821). Cell death was assessed by Annexin-V staining using flow cytometry. Statistical analysis was performed using the Mann–Whitney test. Middle and right panels: *TP53*+/+ (n = 2) and *TP53*−/− (n = 2) clones from NCI-H929, as well as *TP53*+/+ (n = 2), *TP53*−/− (n = 2) and *TP53*R175H/R175H (n = 3) clones from XG7, were treated for 72 h with or without 200 nM STP-B and/or 2.5 μM VE-821, and cell death was assessed with Annexin-V staining using flow cytometry. The data represents the results of two independent experiments. Statistical analyses were performed using the Mann–Whitney test. **(B)** STP-B and VE-821 combination highly synergizes in *TP53*abnormal isogenic clones. Left panel: *TP53*+/+ (n = 2) and *TP53*−/− (n = 2) clones from NCI-H929, as well as *TP53*+/+ (n = 2), *TP53*−/− (n = 2), and *TP53*R175H/R175H (n = 3) clones from XG7, were treated for 72 h with increasing concentrations of STP-B (100, 200, and 500 nM) and/or VE-821 (1.25, 2.5, or 5 μM). Cell death was assessed using Annexin-V staining (left panels). Right panel: Bliss synergy scores were calculated using SynergyFinder. Data represent the mean ± SD of two to three experiments. **(C)** STP-B and VE-821 combination induces DNA damage. Cells were treated for 48 h with 200 nM STP-B and 2.5 μM VE-821, permeabilized and stained with AF647-conjugated anti-γ-H2AX antibody. Fluorescence was assessed by FACs analysis. Left panel: Data are representative of one experiment. Right panel. The percentage of γ-H2AX-positive cells was determined in two *TP53*+/+ (#1, #2) and two *TP53*−/− (#1, #2) NCI-H929 clones. The graph represents the mean ± SD of three independent experiments. Statistical significance is indicated in the figures with symbols *p < 0.05, **p < 0.01 and ****p < 0.0001. ns, Not significant.
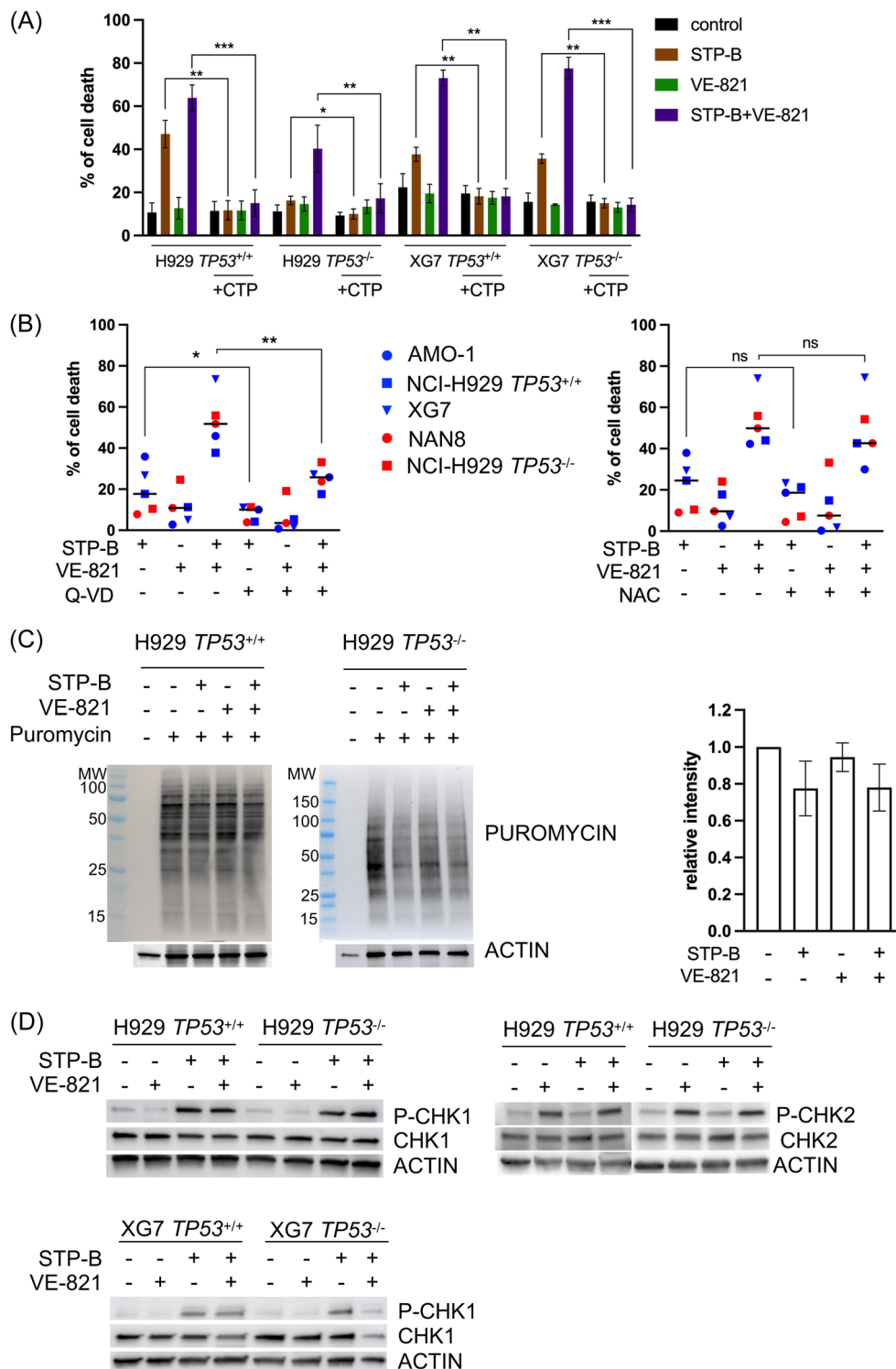
FIGURE 7 Cell death induced by STP-B and VE-821 is strictly dependent on CTP and involves caspase activation. **(A)** The addition of CTP inhibits cell death induced by STP-B alone or in combination with VE-821. Cells were treated for 72 h with 200 nM STP-B, 2.5 μM VE-821, or both, and CTP (200 μM) was added daily to the culture medium. Cell death was assessed by Annexin-V staining using flow cytometry. The graph represents the mean ± SD of three to four independent experiments. Statistical analyses were performed using the paired t-test. **(B)** Cell death induced by STP-B alone or in combination with VE-821 is partly inhibited by the pan-caspase inhibitor Q-VD and not impaired by N-acetyl cysteine (NAC). Cells were treated for 72 h with 200 nM STP-B and 2.5 μM VE-821 alone or in combination with or without 50 μM Q-VD (left panel) or 5 mM NAC (right panel). The graph represents the mean of cell death induced in AMO1, NAN8, NCI-H929 $TP53^{-/-}$, and NCI-H929 $TP53^{+/+}$ and XG7 ($n = 2$ experiments for each cell line and clone). Cell death was assessed by Annexin-V staining using flow cytometry. Statistical analysis was performed using the paired t-test. **(C)** STP-B alone or in combination with VE-821 inhibits protein synthesis. Cells were treated overnight with 200 nM STP-B and 2.5 μM VE-821 alone or in combination, and 1 μM puromycin was added 30 min prior to lysis, protein extraction, and western blotting, as previously described.[22] **(D)** STP-B and VE-821 induce CHK1 and CHK2 phosphorylation. Cells were treated for 24 h with 200 nM STP-B and 2.5 μM VE-821 alone or in combination, prior to lysis, protein extraction, and western blotting. Statistical significance is indicated in the figures with symbols *$p < 0.05$, **$p < 0.01$ and ***$p < 0.001$. ns, Not significant.

(A) Patient samples

(B)

(C) MM xenograft model

FIGURE 8 The inhibition of CTP synthase 1 (CTPS1) and ATR is synergistic in p53-deficient myeloma cells ex vivo and in vivo. **(A)** The STP-B and VE-821 combination is efficient in del17p patient samples. Bone marrow (n = 15) or peripheral blood (n = 2) samples from patients with multiple myeloma at different stages (n = 5 diagnosis, n = 6 relapse, or n = 6 resistant/refractory) were treated for 72 h with 200 nM STP-B, 2.5 µM VE-821, or both. Cell death was assessed by the loss of CD138 staining using flow cytometry. Left panel: The graph represents the results in the 17 samples. **(B)** The graph represents the results in 15 samples according to their del17p status. Statistical analyses were performed using the Friedman test with Dunn's multiple comparisons test (left panel) or the Mann–Whitney test and paired t-test (right panel). **(C)** STP-B and ATR inhibitor AZD6738 prevent NCI-H929 $TP53^{-/-}$ cell growth in NSG mice. NSG mice were subcutaneously injected with 10^6 NCI-H929 $TP53^{-/-}$ cells (left panel). After 1 week, mice with detectable tumors were randomly distributed into four groups of seven mice and treated with STP-B (30 mg/kg), AZD6738 (25 mg/kg), or both, as indicated by the arrows (middle panel). The graphs represent the tumor volume kinetics (mean ± SD, middle panel) and the tumor volume on Day 12 (right panel). Statistical analyses were performed using the two-way analysis of variance with Tukey's multiple comparisons (middle graph) or the Mann–Whitney test (right graph). Statistical significance is indicated in the figures with symbols *p < 0.05, **p < 0.01 and ***p < 0.001. ns, Not significant; NSG, NOD-scid IL2Rgamma.

selective vulnerability. *CTPS1* appears, therefore, to be a very interesting target for patients with a high-risk presentation, that is, proliferation index with or without *TP53* hits.

In vitro, the *CTPS1* expression was similar in $TP53^{abnormal}$ and $TP53^{wt}$ HMCLs, and in isogenic $TP53^{+/+}$, $TP53^{-/-}$, and $TP53^{R175H/R175H}$ clones as well, confirming that *CTPS1* expression was not under p53 control. By using the CTPS1 pharmacological inhibitor STP-B, we showed that STP-B induced cell cycle arrest in the early S phase and synergized with the ATR inhibitor VE-821 in $TP53^{wt}$ and $TP53^{abnormal}$ myeloma cell lines: this combination was efficient irrespective of p53 expression and function, whereas a single hit in *TP53* induced resistance to chemotherapeutical agents, with this resistance being increased by biallelic hit.[35] Of note, we had previously found that isogenic $TP53^{-/-}$ myeloma cells were 5–10-fold more resistant to BH3 mimetics than $TP53^{wt}$, the resistance being caused by the decrease in BAX expression and subsequently in the amount of MCL1/BAX complexes in $TP53^{-/-}$ cells.[27] Our current results show that cell death induced by the combined inhibition of CTPS1 and ATR overcomes the p53-mediated apoptosis resistance and was independent of BAX expression (data not shown). These results clearly show that the CTPS1/ATR inhibition-induced cell death is independent of p53-BAX deficiency, which mediates treatment resistance. Such a combination might be of interest to p53-deficient patients for whom there is still an unmet medical need.

We confirmed the high STP-B specificity to inhibit CTP synthesis by showing that CTP complementation totally inhibited cell death by STP-B with or without VE-821. The effectiveness of STP-B in preventing tumor growth in vivo suggests that tumor dependency on CTP synthesis is not overcome by the tumor microenvironment.

The STP-B and VE-821 combination induced replicative stress with strong phosphorylation of CHK1 and CHK2, indicating activation of the ATR and ATM pathways, which has recently been reported in glioma upon CTP deprivation.[36] It will be interesting to further decipher the signaling cascades induced by CTP deprivation in combination with inhibition of ATR, ATM, or DNA-PK.

As regards, the mechanism of cell death, the lack of impact of NAC addition on cell death rules out a major role for ROS and ferroptosis, while the 50% inhibition of cell death induced by Q-VD indicates an involvement of caspases and suggests activation of apoptosis. Moreover, STP-B decreases protein translation, which impairs the synthesis of short half-life proteins such as MCL1, which is a major survival protein in myeloma.[22,37]

Ex vivo, combination was particularly efficient in samples from refractory/resistant patients and/or from patients with high-risk features such as del17p and/or leukemic stage. Although the number of samples from high-risk patients in this study was limited (n = 5), our results argue for further evaluation of the combination in this patient group. In vivo, in mice, we showed that the combination of STP-B and

TABLE 2 Characteristics of patient samples.

Characteristics of patient samples						Myeloma cell death (%)		
Samples	Disease	Stade	17p	Cytogenetic	CD138 (%)	VE-821	STP-B	Combo
MM#1	MM	D		t(4;14)	43.0	17.1	0	3
MM#2	MM	D		ND	9.0	0	0	0
MM#3	MM	D		ND	4.5	5.2	0	5.8
MM#4	MM	D	ND	t(4;14)⁻	28.0	28.7	5.5	18.3
MM#5	MM	D		t(11;14)⁻ t(4;14)⁻	38.0	15.7	0	35.1
MM#6	MM	R		t(4;14)	3.5	0	0	0
MM#7	MM	R		t(11;14)	5.5	12.7	8.1	15.0
MM#8	MM	R	del17p	t(11;14)⁻ t(4;14)⁻	30.0	15.8	11.2	35.8
MM#9	MM	R		t(11;14)	35.0	0	0	0
MM#10	MM	R		t(11;14)	16.0	7	0.5	9.1
MM#11	MM	R	del17p	t(11;14)⁻ t(4;14)⁻	6.0	0	24.9	42.9
MM#12	MM	RR		ND	22.0	16.0	7.3	19.6
MM#13	MM	RR	ND	ND	35.0	0	4.9	7.4
MM#14	MM	RR		t(11;14)⁻	20.0	12.6	0.6	43.7
MM#15	MM	RR	del17p	ND	43.0	17.6	2.2	33.5
PCL#1	PCL	RR	del17p	t(14;20)	95.0	8.2	8.4	59.9
PCL#2	PCL	RR	del17p	ND	10.0	20.4	8.9	58

Note: Bone marrow or peripheral blood samples were collected from patients with MM or PCL, respectively. Chromosomal abnormalities (del17p and translocation) were assessed by fluorescence in situ hybridization. Myeloma cells were identified by CD138 staining with flow cytometry. Cell death was determined by the loss of CD138+ cells after 72 h of culture with or without STP-B (200 nM) and/or VE-821 (2.5 μM).

Abbreviations: D, diagnosis; MM, multiple myeloma; ND, not determined; PCL, plasma cell leukemia; R, relapse; RR, refractory/resistant.

AZD6738 was well-tolerated, and it strongly inhibited the growth of NCI-H929 *TP53*⁻/⁻ cells. The efficacy of STP-B, in vivo, is under evaluation in several clinical trials. Although ATR is a well-known, not-new target for cancer therapy, the efficacy of its inhibition in vivo has been reported quite recently.[38] Several recent clinical trials assessing the tolerance of ATR inhibitors as single agents have reported good tolerance and even some antitumor efficacy.[39,40] However, the efficacy of ATR inhibition is clearly increased in combination with drugs that interfere with DNA replication or repair. We, and others, have previously reported that ATR inhibitors synergized with chemotherapies such as melphalan, to induce mitotic catastrophe in p53-deficient myeloma cells.[32,41] While melphalan has wide-ranging side effects, STP-B is unlikely to be toxic to normal nonlymphoid cells since they do not express CTPS1, but CTPS2, against which STP-B is not effective. The combination of ATR inhibitors with the dual inhibition of CTPS1 and CTPS2 was reported to induce synthetic lethality in MYC-overexpressing cell lines, confirming the interest in targeting CTPS1 and ATR in cancer.[42] Inhibitors targeting other kinases involved in the replication stress (CHK1 and WEE1) were also shown to synergistically induce cell death with STP-B in myeloma cell lines.[21] Inhibiting ATR appears particularly attractive in myeloma because *ATR* is well-expressed, rarely deleted or mutated in patient samples at diagnosis or in HMCLs (which are derived from patients with the most aggressive presentation, i.e., extramedullary disease), and is expressed in patient samples with high-risk features (high proliferation and/or low p53 score). Although we cannot rule out that the combined efficacy of STP-B and ATR inhibitors ex vivo in patient samples may be, at least partially, related to the inhibition of STP-B-induced protein synthesis, which decreases the expression of critical proteins with short half-life, such as MCL1 or CCND1, it seems unlikely that the combination with ATR inhibitors involved such mechanisms to induce cell death.[22] Nevertheless, multivariate analysis

showed that the *CTPS1* expression was predictive of reduced overall survival independently of *MKI67* expression, suggesting that CTPS1 has other impacts than DNA synthesis on myeloma escape to therapies.

To summarize, our results show that the dual-targeting of CTPS1 and ATR induces mitotic catastrophe in p53-deficient patient myeloma cells and cell lines. This provides a rationale for developing therapies for refractory/resistant myeloma patients with *TP53* deficiency, who can be identified using an 8-gene p53 score or *CTPS1* expression, and for whom there is still an unmet clinical need.

AUTHOR CONTRIBUTIONS

Romane Durand: Conceptualization; formal analysis; investigation; writing—original draft preparation. **Céline Bellanger**: Software; formal analysis. **Géraldine Descamps**: Investigation. **Christelle Dousset**:

investigation. **Sophie Maïga**: Investigation. **Jennifer Derrien**: Software; formal analysis. **Laura Thirrourad**: Investigation. **Louise Bouard**: Conceptualization. **Patricia Gomez-Bougie**: Writing—review and editing. **Marie-Claire Devilder**: Methodology. **Hélène Asnagli**: Resources. **Andrew Parker**: Resources. **Philip Beer**: Resources; conceptualization. **Philippe Moreau**: Funding acquisition; resources. **Cyrille Touzeau**: Funding acquisition; resources. **Agnès Moreau-Aubry**: Methodology. **David Chiron**: Conceptualization; writing—review and editing. **Catherine Pellat-Deceunynck**: Supervision; conceptualization; formal analysis; investigation; writing—original draft preparation.

CONFLICT OF INTEREST STATEMENT

DATA AVAILABILITY STATEMENT

Data that support the findings of this study are available from the corresponding author upon reasonable request.

FUNDING

ORCID

Romane Durand http://orcid.org/0000-0002-5422-0362
Géraldine Descamps http://orcid.org/0009-0007-3933-1834
Patricia Gomez-Bougie http://orcid.org/0000-0002-4846-4782
Agnès Moreau-Aubry http://orcid.org/0000-0001-5540-3374
David Chiron http://orcid.org/0000-0002-2199-752X
Catherine Pellat-Deceunynck http://orcid.org/0000-0002-6287-8148

SUPPORTING INFORMATION

Additional supporting information can be found in the online version of this article.

REFERENCES

1. Moreau P, Attal M, Hulin C, et al. Bortezomib, thalidomide, and dexamethasone with or without daratumumab before and after autologous stem-cell transplantation for newly diagnosed multiple myeloma (CASSIOPEIA): a randomised, open-label, phase 3 study. *Lancet*. 2019;394(10192):29-38.
2. Moreau P, Garfall AL, van de Donk NWCJ, et al. Teclistamab in relapsed or refractory multiple myeloma. *N Engl J Med*. 2022;387(6):495-505.
3. Berdeja JG, Madduri D, Usmani SZ, et al. Ciltacabtagene autoleucel, a B-cell maturation antigen-directed chimeric antigen receptor T-cell therapy in patients with relapsed or refractory multiple myeloma (CARTITUDE-1): a phase 1b/2 open-label study. *Lancet*. 2021;398(10297):314-324.
4. Munshi NC, Anderson LD, Shah N, et al. Idecabtagene vicleucel in relapsed and refractory multiple myeloma. *N Engl J Med*. 2021;384(8):705-716.
5. Manier S, Ingegnere T, Escure G, et al. Current state and next-generation CAR-T cells in multiple myeloma. *Blood Rev*. 2022;54:100929.
6. Corre J, Perrot A, Caillot D, et al. del(17p) without *TP53* mutation confers a poor prognosis in intensively treated newly diagnosed patients with multiple myeloma. *Blood*. 2021;137(9):1192-1195.
7. Ansari-Pour N, Samur M, Flynt E, et al. Whole-genome analysis identifies novel drivers and high-risk double-hit events in relapsed/refractory myeloma. *Blood*. 2023;141(6):620-633.
8. Tessoulin B, Eveillard M, Lok A, et al. p53 dysregulation in B-cell malignancies: more than a single gene in the pathway to hell. *Blood Rev*. 2017;31(4):251-259.
9. Kruiswijk F, Labuschagne CF, Vousden KH. p53 in survival, death and metabolic health: a lifeguard with a licence to kill. *Nat Rev Mol Cell Biol*. 2015;16(7):393-405.
10. Lok A, Descamps G, Tessoulin B, et al. p53 regulates CD46 expression and measles virus infection in myeloma cells. *Blood Adv*. 2018;2(23):3492-3505.
11. Tessoulin B, Descamps G, Dousset C, Amiot M, Pellat-Deceunynck C. Targeting oxidative stress with auranofin or Prima-1Met to circumvent p53 or Bax/Bak deficiency in myeloma cells. *Front Oncol*. 2019;9:128.
12. Saldivar JC, Hamperl S, Bocek MJ, et al. An intrinsic S/G2 checkpoint enforced by ATR. *Science*. 2018;361(6404):806-810.
13. Galluzzi L, Vitale I, Aaronson SA, et al. Molecular mechanisms of cell death: recommendations of the Nomenclature Committee on Cell Death 2018. *Cell Death Differ*. 2018;25(3):486-541.
14. Toledo LI, Altmeyer M, Rask M-B, et al. ATR prohibits replication catastrophe by preventing global exhaustion of RPA. *Cell*. 2013;155(5):1088-1103.
15. Da Costa AABA, Chowdhury D, Shapiro GI, D'Andrea AD, Konstantinopoulos PA. Targeting replication stress in cancer therapy. *Nat Rev Drug Discov*. 2023;22(1):38-58.
16. Martin E, Palmic N, Sanquer S, et al. CTP synthase 1 deficiency in humans reveals its central role in lymphocyte proliferation. *Nature*. 2014;510(7504):288-292.
17. Martin E, Minet N, Boschat A-C, et al. Impaired lymphocyte function and differentiation in CTPS1-deficient patients result from a hypomorphic homozygous mutation. *JCI Insight*. 2020;5(5):e133880.
18. Minet N, Boschat A-C, Lane R, et al. Differential roles of CTP synthetases CTPS1 and CTPS2 in cell proliferation. *Life Sci Alliance*. 2023;6(9):e202302066.
19. Liang JH, Ren YM, Du KX, et al. MYC-induced cytidine metabolism regulates survival and drug resistance via cGas-STING pathway in mantle cell lymphoma. *Br J Haematol*. 2023;202(3):550-565.
20. Soudais C, Schaus R, Bachelet C, et al. Inactivation of cytidine triphosphate synthase 1 prevents fatal auto-immunity in mice. *Nat Commun*. 2024;15(1):1982.
21. Pfeiffer C, Grandits AM, Asnagli H, et al. CTPS1 is a novel therapeutic target in multiple myeloma which synergizes with inhibition of CHEK1, ATR or WEE1. *Leukemia*. 2024;38(1):181-192.
22. Durand R, Bellanger C, Kervoëlen C, et al. Selective pharmacologic targeting of CTPS1 shows single-agent activity and synergizes with BCL2 inhibition in aggressive mantle cell lymphoma. *Haematologica*. 2024;109(8):2574-2584. doi:10.3324/haematol.2023.284345
23. Benaniba L, Tessoulin B, Trudel S, et al. The MYRACLE protocol study: a multicentric observational prospective cohort study of patients with multiple myeloma. *BMC Cancer*. 2019;19(1):855.
24. Gomez-Bougie P, Maiga S, Tessoulin B, et al. BH3-mimetic toolkit guides the respective use of BCL2 and MCL1 BH3-mimetics in myeloma treatment. *Blood*. 2018;132(25):2656-2669.
25. Tessoulin B, Moreau-Aubry A, Descamps G, et al. Whole-exon sequencing of human myeloma cell lines shows mutations related to myeloma patients at relapse with major hits in the DNA regulation and repair pathways. *J Hematol Oncol*. 2018;11(1):137.
26. Maïga S, Brosseau C, Descamps G, et al. A simple flow cytometry-based barcode for routine authentication of multiple myeloma and mantle cell lymphoma cell lines. *Cytometry A*. 2015;87(4):285-288.
27. Durand R, Descamps G, Bellanger C, et al. A p53 score derived from *TP53* CRISPR/Cas9 HMCLs predicts survival and reveals a major role of BAX in the response to BH3 mimetics. *Blood*. 2024;143(13):1242-1258.
28. Asnagli H, Minet N, Pfeiffer C, et al. CTP synthase 1 is a novel therapeutic target in lymphoma. *HemaSphere*. 2023;7(4):e864.

29. Novak A, Laughton D, Lane R, et al. Discovery and optimization of potent and orally available CTP synthetase inhibitors for use in treatment of diseases driven by aberrant immune cell proliferation. *J Med Chem*. 2022;65(24):16640-16650.

30. Alberge J-B, Kraeber-Bodéré F, Jamet B, et al. Molecular signature of ^{18}F-FDG PET biomarkers in newly diagnosed multiple myeloma patients: a genome-wide transcriptome analysis from the CASSIOPET study. *J Nucl Med*. 2022;63(7):1008-1013.

31. Foroutan M, Bhuva DD, Lyu R, Horan K, Cursons J, Davis MJ. Single sample scoring of molecular phenotypes. *BMC Bioinformatics*. 2018;19(1):404.

32. Botrugno OA, Bianchessi S, Zambroni D, et al. ATR addiction in multiple myeloma: synthetic lethal approaches exploiting established therapies. *Haematologica*. 2019;105(10):2440-2447.

33. Reaper PM, Griffiths MR, Long JM, et al. Selective killing of ATM- or p53-deficient cancer cells through inhibition of ATR. *Nat Chem Biol*. 2011;7(7):428-430.

34. Foote KM, Lau A, Nissink JWM. Drugging ATR: progress in the development of specific inhibitors for the treatment of cancer. *Future Med Chem*. 2015;7(7):873-891.

35. Munawar U, Roth M, Barrio S, et al. Assessment of TP53 lesions for p53 system functionality and drug resistance in multiple myeloma using an isogenic cell line model. *Sci Rep*. 2019;9(1):18062.

36. Hathaway MR, Gadek KE, Jagana HL, et al. CTPS1 inhibition synergizes with replication stress signaling inhibition in MYC -amplified Group 3 medulloblastoma. *bioRxiv*. 2024. doi:10.1101/2024.06.03.597242

37. Gomez-Bougie P, Ménoret E, Juin P, Dousset C, Pellat-Deceunynck C, Amiot M. Noxa controls Mule-dependent Mcl-1 ubiquitination through the regulation of the Mcl-1/USP9X interaction. *Biochem Biophys Res Commun*. 2011;413(3):460-464.

38. Karnitz LM, Zou L. Molecular pathways: targeting ATR in cancer therapy. *Clin Cancer Res*. 2015;21(21):4780-4785.

39. Yap TA, O'Carrigan B, Penney MS, et al. Phase I trial of first-in-class ATR inhibitor M6620 (VX-970) as monotherapy or in combination with carboplatin in patients with advanced solid tumors. *J Clin Oncol*. 2020;38(27):3195-3204.

40. Terranova N, Jansen M, Falk M, Hendriks BS. Population pharmacokinetics of ATR inhibitor berzosertib in phase I studies for different cancer types. *Cancer Chemother Pharmacol*. 2021;87(2):185-196.

41. Bouard L, Tessoulin B, Descamps G, et al. Inhibition of ATR overcomes chemotherapy resistance in p53 deficient myeloma cells. *Blood*. 2019;134(Suppl_1):3109.

42. Sun Z, Zhang Z, Wang Q-Q, Liu J-L. Combined inactivation of CTPS1 and ATR is synthetically lethal to MYC-overexpressing cancer cells. *Cancer Res*. 2022;82(6):1013-1024.